SLAC-PUB-5145
December 1989
(M)

$s\bar{s}$ SPECTROSCOPY FROM THE LASS SPECTROMETER*

D. ASTON,[1] N. AWAJI,[2] T. BIENZ,[1] F. BIRD,[1] J. D'AMORE,[3]
W. DUNWOODIE,[1] R. ENDORF,[3] K. FUJII,[2] H. HAYASHII,[2] S. IWATA,[2]
W. JOHNSON,[1] R. KAJIKAWA,[2] P. KUNZ,[1] D. LEITH,[1] L. LEVINSON,[1]
T. MATSUI,[2] B. MEADOWS,[3] A. MIYAMOTO,[2] M. NUSSBAUM,[3] H. OZAKI,[2]
C. PAK,[2] B. RATCLIFF,[1] D. SCHULTZ,[1] S. SHAPIRO,[1] T. SHIMOMURA,[2]
P. SINERVO,[1] A. SUGIYAMA,[2] S. SUZUKI,[2] G. TARNOPOLSKY,[1]
T. TAUCHI,[2] N. TOGE,[1] K. UKAI,[4] A. WAITE,[1] S. WILLIAMS[1]

[1]*Stanford Linear Accelerator Center, Stanford University, Stanford, CA 94309*
[2]*Nagoya University, Department of Physics, Nagoya-Shi 461, Japan*
[3]*University of Cincinnati, Cincinnati, OH 45221*
[4]*Institute for Nuclear Study, University of Tokyo, Tokyo 188, Japan*

A brief summary is presented of results pertinent to $s\bar{s}$ spectroscopy derived from high statistics data on $K^- p$ interactions obtained with the LASS spectrometer at SLAC.

1. INTRODUCTION

This paper summarizes recent results on $s\bar{s}$ spectroscopy obtained from an exposure of the Large Aperture Superconducting Solenoid (LASS) spectrometer at SLAC to a K^- beam of 11 GeV/c. The spectrometer and relevant experimental details are described elsewhere.[1,2] The raw data sample contains $\sim$ 113 million triggers, and the resulting useful beam flux corresponds to a sensitivity of 4.1 events/nb. The acceptance is approximately uniform over almost the full 4π solid angle.

Invited talk presented at the IX European Symposium on Antiproton-Proton Interactions, Mainz, Germany, September 5–10, 1988; also published in Nuclear Physics B (Proc. Suppl.) **8** *(1989) 32–39.*

⋆ Work supported by Department of Energy contract DE–AC03–76SF00515; the National Science Foundation under grants PHY82–09144 and PHY85–13808; and the Japan–US Cooperative Research Project on High Energy Physics.

2. $s\bar{s}$ SPECTROSCOPY

A principal objective in studying meson spectroscopy is the precise definition of the level structure of the anticipated $q\bar{q}$ meson states. The quark model level diagram is expected to take the form[3] illustrated qualitatively in Fig. 1 for the charmonium states.[4] Here S and L denote total quark spin and orbital angular momentum, respectively, and C indicates the charge conjugation parity of the resulting meson state. The paracharmonium levels are singlets, whereas the orthocharmonium levels, other than ^{3}S, are triplets separated in mass due to spin–orbit interaction. Within each column, the lowest-lying state is the ground state, and the higher states correspond to radial excitations of this state. The leading orbital excitations are the ground states with largest total angular momentum, J, and, for the triplet levels, the remaining states are termed the underlying states. In e^+e^- collisions, the ^{3}S tower of states is readily accessible, while information on the leading orbital excitations with $J \geq 3$ is lacking, and that on the corresponding underlying states is sparse. Results of a complementary nature are obtained from hadronic interaction experiments, where production of the leading orbital states predominates, and information on the underlying and radially excited states requires careful amplitude analyses of high statistics data.

The present experiment provides such data on the mainly $s\bar{s}$ meson states. The resulting light quark level structure is related to the nature of the long-range (i.e., confining) part of the $q\bar{q}$ interaction, and thus, in principle, provides information on nonperturbative QCD. In practice, it enables us to learn about QCD potential models incorporating relativistic corrections.[5]

The processes most relevant to the study of $s\bar{s}$ (i.e., strangeonium) spectroscopy are those in which a $K\overline{K}$ or $K\overline{K}\pi$ system is produced against a recoil hyperon. However, in recent years candidate glueball states which also couple to these meson systems have emerged from the study of J/ψ decay. Consequently, it has become increasingly important to define the quark model level structure in order to distinguish those states which may be of different dynamical origin. In the present experiment, the relevant reactions which have been studied are:

$$K^- p \to K^0_S K^0_S \Lambda_{seen} \quad , \tag{1}$$

$$K^- p \to K^- K^+ \Lambda_{seen} \quad , \tag{2}$$

and

$$K^- p \to K^0_S K^\pm \pi^\mp \Lambda_{seen} \quad . \tag{3}$$

They are characterized by peripheral (i.e., quark exchange) production of the meson system, and it follows that the creation of glueball states should be disfavored in such processes. The corresponding data samples are very clean, and amplitude analyses have been performed,[2,6–8] the results of which are summarized here.

The raw $K\overline{K}$ mass distributions for reactions (1) and (2) (Fig. 2) differ, since for the former only even spin states are produced. In addition, for reaction (2), the mass region above $\sim$ 1.7 GeV/c^2 is dominated by the reflection of diffractive production of low mass ΛK^+ systems.[9] In Fig. 3, the $K^0_S K^0_S$ mass spectrum from reaction (1) is compared to the MARK III data on radiative J/ψ decay[10] in the mass region below 1.9 GeV/c^2 [the LASS data have been scaled to the MARK III data at the peak of the $f_2'(1525)$]. Both spectra show a small but intriguing threshold rise,[2,11] followed by activity in the $f_2(1270)/a_2(1320)$ region and then the large $f_2'(1525)$ peak. At higher mass, the MARK III spectrum is dominated by the $f_2(1720)$. There is no evidence for any such signal in the LASS distribution, and the upper limit on the production cross section is 94 nb at the 95% confidence level; it should be noted also that there is no evidence for $f_2(1720)$ production in reaction (3) in the present experiment[6] [cf. Fig. 9(f)]. These results indicate that the $f_2(1720)$ is indeed a strong candidate glueball state.

The amplitude analysis of reaction (1)[2] yields the S-wave intensity distribution of Fig. 4(a). Although the uncertainties are large, the data seem to peak in the range $\sim$ 1.5–1.6 GeV/c^2. A similar distribution [Fig. 4(b)] has been obtained in an analysis of reaction (2) at 8.25 GeV/c,[12] and there are indications of S-wave structure at this mass from the data on reaction (2) in the present experiment. These results suggest the existence of a 0^+ state in this mass region which is naturally interpreted

as a partner of the $f_2'(1525)$ in the ^{3}P ground state. It is not clear whether this state might be identified with the $f_0(1590)$.[13] An immediate consequence of this observation is that the $f_0(975)$, which is usually assigned to this multiplet, may well be a weakly bound $K\overline{K}$ system,[14] or be of some other non-$q\,\overline{q}$ origin. This is discussed at greater length in Ref. 2.

For the $K\overline{K}$ system in reaction (2), the acceptance-corrected spherical harmonic moments ($t_{\rm L}^{\rm M} = \sqrt{4\pi}{\rm N}\langle {\rm Y_{LM}}\rangle$; L $\leq$ 8, M = 0) in the t-channel helicity frame are shown in Fig. 5 for the mass region 1.68–2.44 GeV/c^2, and $t' \leq 0.2$ (GeV/c)^2. It should be noted that amplitudes with spin J can contribute to moments with L $\leq 2J$. There is a peak in the mass spectrum, t_0^0, at $\sim$ 1.86 GeV/c^2, and similar structure is present for all moments with L $\leq$ 6, but is absent for L $\geq$ 7. This, together with the absence of such a signal for reaction (1),[2] indicates the presence of a $J^{\rm PC} = 3^{--}$, mostly $s\,\overline{s}$ state. A detailed analysis of this region[7] yields the total F-wave intensity distribution of Fig. 6(a) for $t' \leq 1.0$ (GeV/c)^2; the fitted curve gives BW mass and width 1855 $\pm$ 22 and 74 $\pm$ 67 MeV/c^2, respectively. A similar fit to the mass spectrum [Fig. 6(b)] gives parameter values 1851 $\pm$ 9 and 66 $\pm$ 29 MeV/c^2, in agreement with previous measurements from the mass distribution only.[15,16] It should be noted that the spin of this state, which is listed as the $\phi_{\rm J}(1850)$,[4] is established by the LASS data, and that the mass and width have been estimated for the first time on the basis of an amplitude analysis.

A significant $J^{\rm P} = 3^-$ signal [Fig. 9(g)] has been obtained in the $\phi_3(1850)$ region from the partial wave analysis of reaction (3).[6] This signal, after all corrections, is shown in Fig. 6(c) (open dots) in comparison with that from reaction (2) (solid dots); the branching ratio obtained is $BR[(\phi_3(1850) \rightarrow (K^*\overline{K} + c.c.))/(\phi_3(1850) \rightarrow K\overline{K})] = 0.55^{+0.85}_{-0.45}$, in agreement with theory.[5]

The $\phi_3(1850)$ is interpreted as belonging to the $^3{\rm D}_3$ quark model nonet which also includes the $\rho_3(1690)$, the $\omega_3(1670)$, and the $K_3^*(1780)$. Using current mass values,[4] the mass formula[17] yields an octet-singlet mixing angle of $\sim 30°$. This indicates that the multiplet is almost ideally mixed, and that the $\phi_3(1850)$ is an almost pure $s\,\overline{s}$ state, in accord with its production characteristics.

The analysis of the ϕ_3 region[7] has shown that the peaks observed in Fig. 5 are due to interference between the resonant F-wave and the approximately imaginary amplitude describing the diffractive production of the low mass ΛK^+ system. In Fig. 5, there is also a small signal in every moment with L $\geq$ 1 at $\sim$ 2.2 GeV/c^2; no such signal is observed for L $\geq$ 9. This indicates the existence at this mass of a small, resonant 4^+ amplitude which interferes with the large, imaginary, diffractive background, just as for the ϕ_3. An analysis based on this interpretation[8] yields mass and width values of 2209^{+17}_{-15} and 60^{+107}_{-57} MeV/c^2 for this $J^{PC} = 4^{++}$ state. These values are consistent with those obtained by MARK III for the $X(2220)$,[10] and with a signal in the $\eta\eta'$ mass spectrum observed by the GAMS collaboration.[18] The $K\overline{K}$ mass distribution from reaction (1) in this region has been shown[2] to be very similar to that observed for radiative J/ψ decay (Fig. 7), and, in addition, a recent amplitude analysis of the MARK III data has yielded evidence that the $X(2220)$ may indeed have $J^{PC} = 4^{++}$.[19] All this indicates that the $X(2220)$, which has been conjectured to be a glueball state, may instead be a member of the quark model $^3F_4$ ground state nonet.

The raw $K\overline{K}\pi$ mass spectrum for reactions (3) (Fig. 8) exhibits a small signal at the $f_1(1285)$, followed by a rapid rise at $K\overline{K^*}$ threshold to a peak at $\sim$ 1.5 GeV/c^2, and a second peak at $\sim$ 1.9 GeV/c^2. The low mass structure is similar to that observed at 4.2 GeV/c.[20] An amplitude analysis[6] yields the partial wave intensity distributions of Fig. 9. The low mass peak is associated primarily with 1^+ waves, while the 1.9 GeV/c^2 bump is due mainly to the 2^- and the 3^- contribution discussed previously. Only K^* or $\overline{K^*}$ isobar production is important; amplitudes involving the $a_0(980)$ are negligibly small. The 1^+ intensity at low mass shows a pronounced asymmetry in favor of the $\overline{K^*}$ isobar, and also exhibits K^*–$\overline{K^*}$ interference, which is destructive near threshold, and constructive at $\sim$ 1.5 GeV/c^2. This suggests the existence of two 1^+ states of opposite G-parity in this region. The corresponding J^{PG} amplitude combinations yield 1^{++} and 1^{+-} production intensity distributions (Fig. 10) which are well described as BW resonances of mass 1.53 $\pm$ 0.01 and 1.38 $\pm$ 0.02 GeV/c^2, respectively, with corresponding widths of 0.10 $\pm$ 0.04 and 0.08 $\pm$ 0.03 GeV/c^2. The 1^{++} state confirms an earlier observation,[20] while the 1^{+-} state is new. If these are isoscalars,[20] the lower

mass state, the $h_1(1380)$, completes the $J^{PC} = 1^{+-}$ ground state nonet, while the higher mass state, the $f_1(1530)$, is a strong candidate to replace the $E/f_1(1420)$ in the corresponding 1^{++} nonet. Use of the $f_1(1530)$ in this nonet gives a mixing angle $\sim 55°$; this implies that the $f_1(1530)$ is mainly $s\bar{s}$ and that the $f_1(1285)$ has little $s\bar{s}$ content, in agreement with their production characteristics. This is not the case when the E is used, since its production properties are not consistent with the predicted large $s\bar{s}$ content. Finally, a previous analysis[21] of the 1^{++} nonet made use of the E mass and width to predict an a_1 mass of ~ 1.47 GeV/c^2; when the $f_1(1530)$ mass and width are used instead, the predicted mass is ~ 1.28 GeV/c^2, in much better agreement with the accepted value.[4]

The 1^+ states observed in the present experiment satisfactorily complete the ground state $^1P_1$ and $^3P_1$ quark model nonets. Furthermore, the small spin–orbit interaction implied when the new information on the 0^+ is also taken into account contrasts markedly with the corresponding behavior in the charmonium sector. The status of the E meson as a $q\bar{q}$ state is dubious. However, it may be that its proximity to $K\overline{K^*}$ threshold is significant in that it could be a $K\overline{K^*}$ molecule or four-quark state of some kind.

3. CONCLUSION

The present experiment has made significant contributions to the understanding of $s\bar{s}$ spectroscopy. Data analysis is continuing, and further results will be forthcoming on the production of meson systems such as $K^*\overline{K^*}$ against a recoil Λ.

ACKNOWLEDGMENT

We are very grateful for the support of the technical staffs of the collaborating institutions.

REFERENCES

1. D. Aston et al., "The LASS Spectrometer," SLAC–REP–298 (1986).
2. D. Aston et al., *Nucl. Phys.* **B301** (1988) 525.
3. W. Grotrian, *Graphische Darstellung der Spektren von Atomen und Ionen mit ein, zwei und drei Valenzelektronen* (Springer, Berlin, 1928).
4. Particle Data Group, *Phys. Lett.* **170B** (1986).
5. S. Godfrey and N. Isgur, *Phys. Rev.* **D32** (1985) 189.
6. D. Aston et al., *Phys. Lett.* **201B** (1988) 573.
7. D. Aston et al., *Phys. Lett.* **208B** (1988) 324.
8. D. Aston et al., DPNU–88–24 / SLAC–PUB–4661 (1988), to be published in *Phys. Lett. B.*
9. D. Aston et al., SLAC–PUB–4202 / DPNU–87–08 (1987).
10. R. M. Baltrusaitis et al., *Phys. Rev. Lett.* **56** (1986) 107.
11. K. L. Au et al., *Phys. Rev.* **D35** (1987) 1633.
12. M. Baubillier et al., *Z. Phys.* **C17** (1983) 309.
13. D. Alde et al., *Phys. Lett.* **201B** (1988) 160, and references therein.
14. J. Weinstein and N. Isgur, *Phys. Rev. Lett.* **48** (1982) 659; *Phys. Rev.* **D27** (1983) 588, and references therein.
15. S. Al-Harran et al., *Phys. Lett.* **101B** (1981) 357.
16. T. Armstrong et al., *Phys. Lett.* **110B** (1982) 77.
17. M. Gell-Mann, Caltech report TSL–20 (1961) unpublished;
    S. Okubo, *Prog. Theor. Phys.* (Kyoto) **27** (1967) 949.
18. D. Alde et al., *Phys. Lett.* **177B** (1986) 120.
19. T. A. Bolton, Ph. D. thesis, M.I.T. (1988)
20. Ph. Gavillet et al., *Z. Phys.* **C16** (1982) 119.
21. R. K. Carnegie et al., *Phys. Lett.* **68B** (1977) 287.

FIGURE CAPTIONS

1. The quark model level diagram for the charmonium states; the mass scale is only qualitative.
2. The $K\overline{K}$ mass projections for reactions (1) and (2).
3. The comparison of the $K^0_S K^0_S$ mass distribution from reaction (1) with that from radiative J/ψ decay[10] from threshold up to 1.9 GeV/c^2.
4. (a) The S-wave intensity distribution from the amplitude analysis of reaction (1); and (b) the S-wave intensity distribution from the amplitude analysis of reaction (2) at 8.25 GeV/c.[12]
5. The mass dependence of the unnormalized spherical harmonic moments of the K^-K^+ system from reaction (2) in the region 1.68–2.44 GeV/c^2 and $t' \leq 0.2$ (GeV/c)^2.
6. (a) The total F-wave intensity distribution; (b) the corresponding acceptance-corrected mass distribution from reaction (2) for $t' \leq 1.0$ (GeV/c)^2 in the ϕ_3 mass region; and (c) the comparison of the F-wave intensity distributions, after all corrections, from reaction (2) (solid dots) and reactions (3) (open dots). The curves in (a–c) correspond to fits using a BW line shape plus linear background term.
7. The comparison of the $K^0_S K^0_S$ mass distribution from reaction (1) with that from radiative J/ψ decay[10] in the mass range 1.8–2.7 GeV/c^2.
8. The combined raw $K\overline{K}\pi$ mass distributions from reactions (3).
9. The intensity distributions corresponding to the partial wave decomposition for the $K\overline{K}\pi$ system in reactions (3).
10. The production amplitude intensity distributions from reactions (3) for the $K\overline{K^*}$ and $\overline{K}K^*$ G-parity eigenstate combinations; (a–f) are labelled by $J^{\rm PG}{\rm M}^{\eta}$, where M is the helicity and η the naturality of the t-channel exchange.

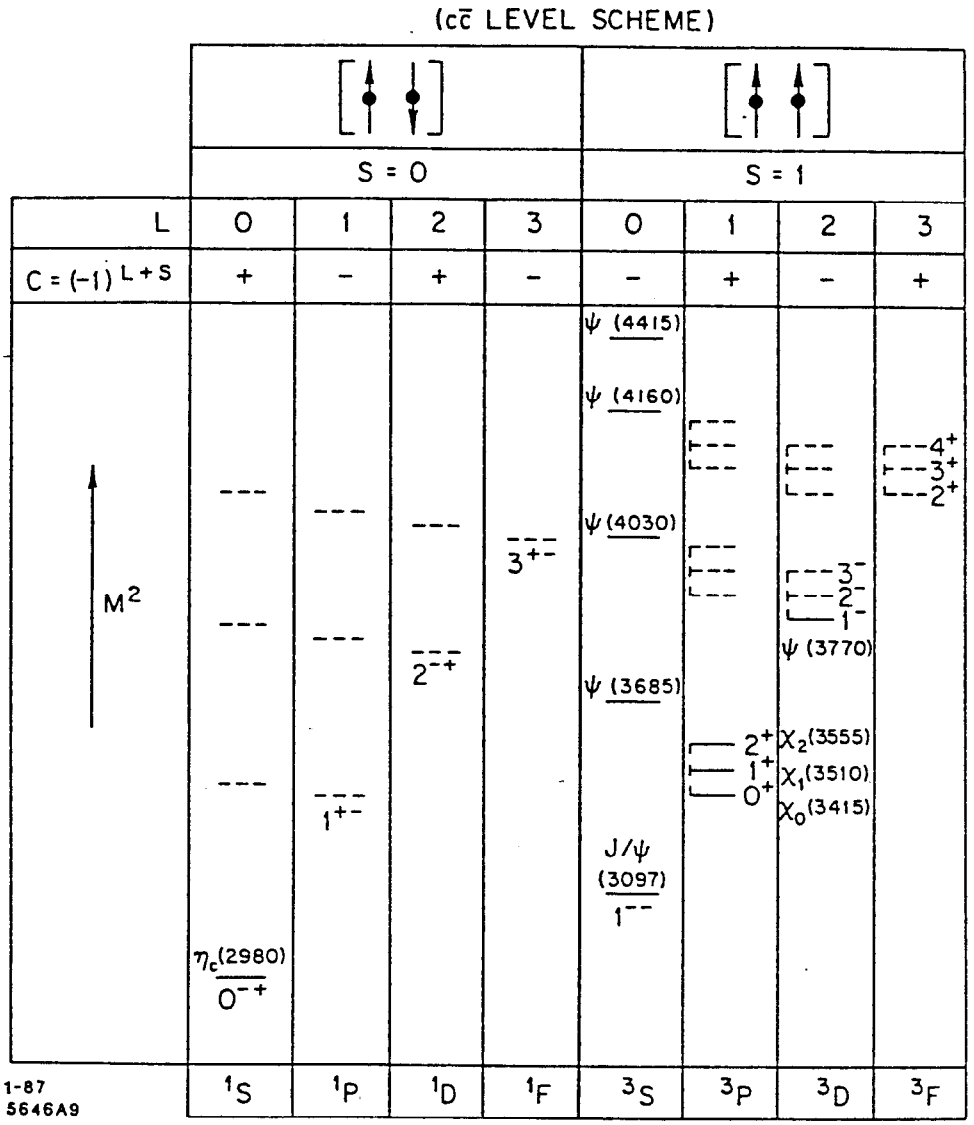
(cc̄ LEVEL SCHEME)
S = 0
S = 1
L
0
1
2
3
0
1
2
3
C = (-1) L+S
+
−
+
−
−
+
−
+
M2
ψ (4415)
ψ (4160)
ψ (4030)
ψ (3685)
J/ψ (3097) 1−−
ηc(2980) 0−+
3+−
2−+
1+−
2+
1+
0+
χ2(3555)
χ1(3510)
χ0(3415)
3−
2−
1−
ψ (3770)
4+
3+
2+
1S
1P
1D
1F
3S
3P
3D
3F
1-87
5646A9

Fig. 1

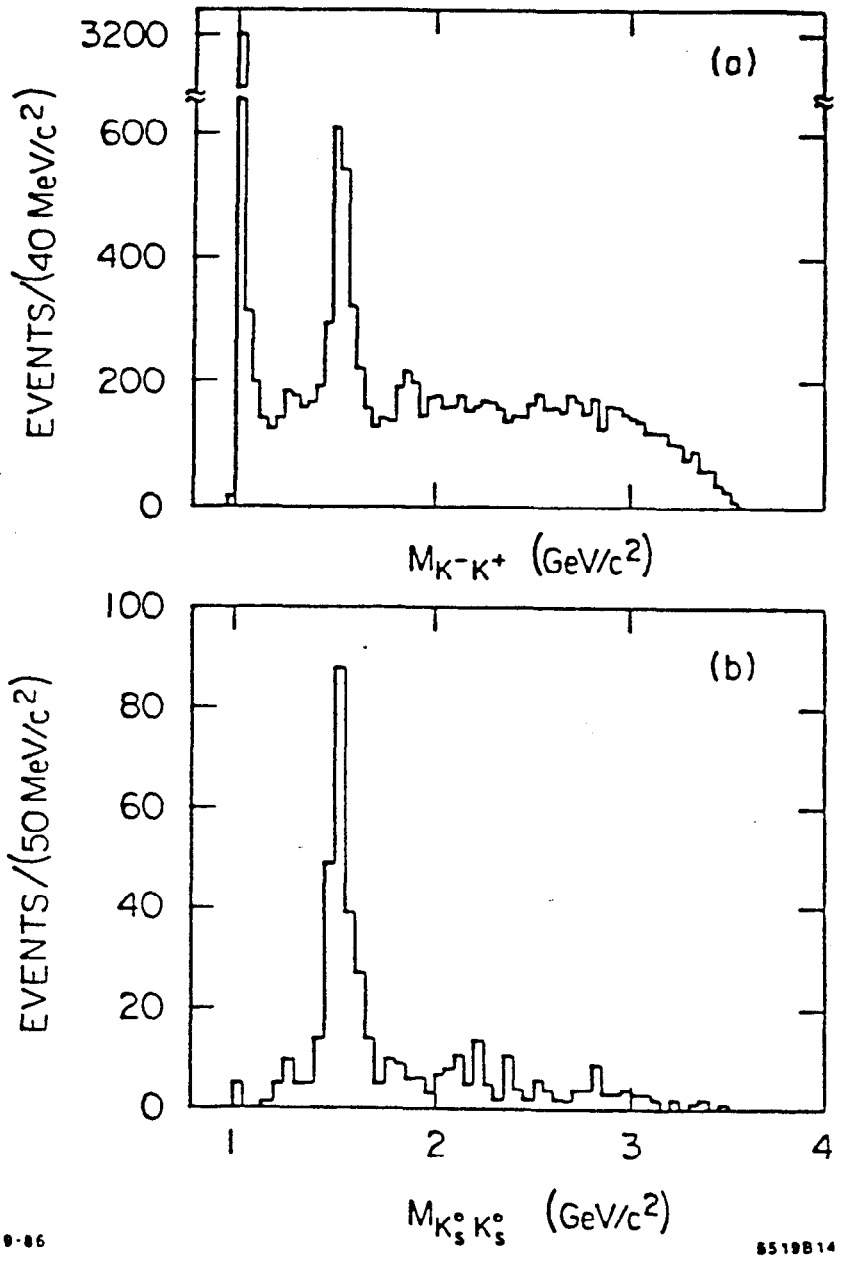
3200
600
400
200
0
EVENTS/(40 MeV/c²)
(a)
$M_{K^-K^+}$ (GeV/c²)
100
80
60
40
20
0
EVENTS/(50 MeV/c²)
(b)
1
2
3
4
$M_{K^0_S K^0_S}$ (GeV/c²)
9-86
8519B14

Fig. 2

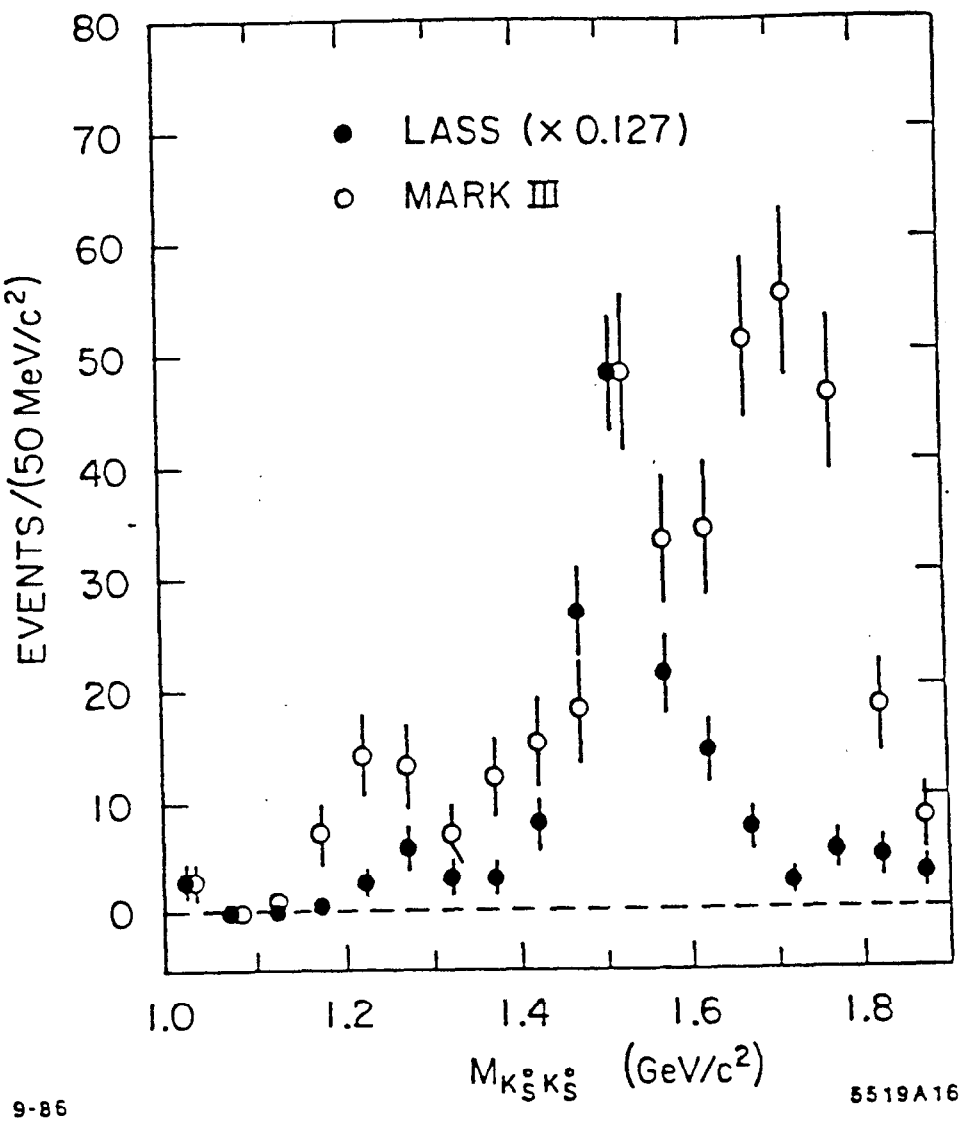
80
70
60
50
40
30
20
10
0
LASS (× 0.127)
MARK III
EVENTS/(50 MeV/c²)
1.0
1.2
1.4
1.6
1.8
$M_{K_S^0 K_S^0}$ (GeV/c²)
9-86
5519A16

Fig. 3

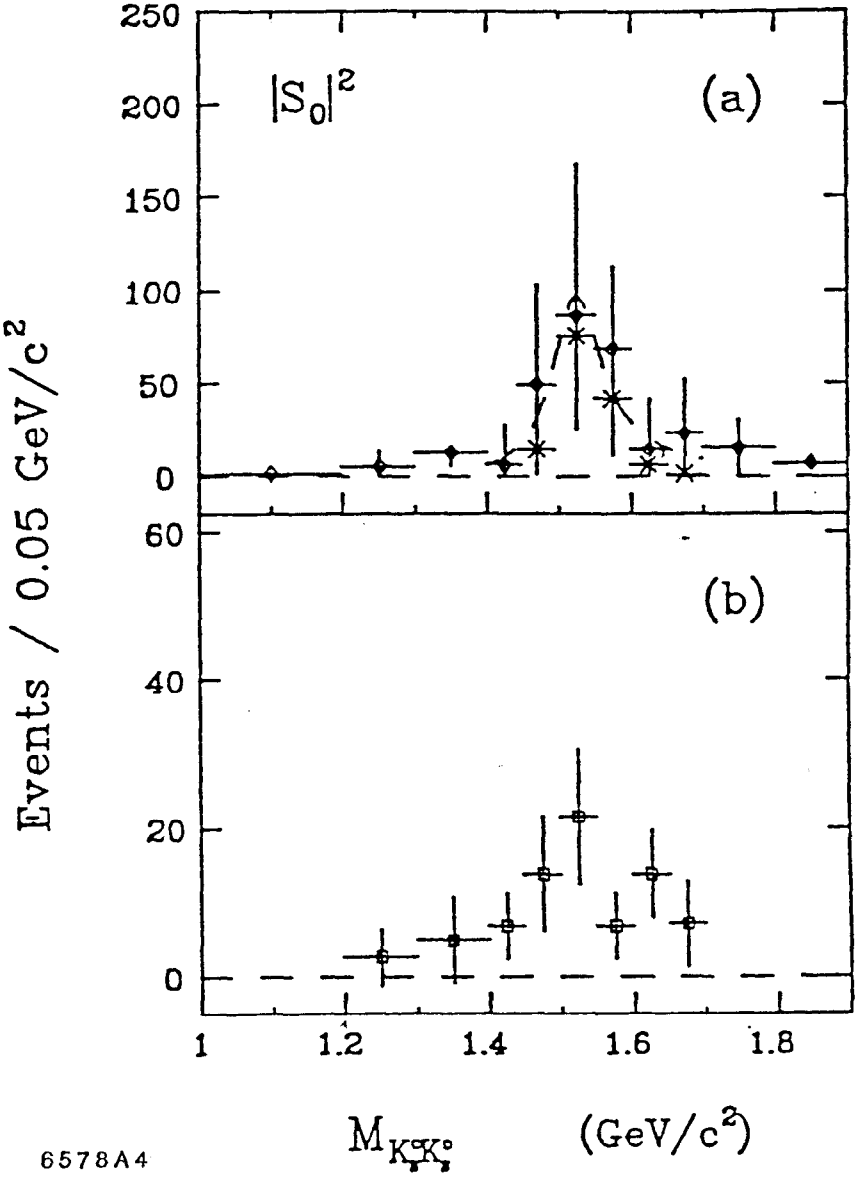
250
200
150
100
50
0
$|S_0|^2$
(a)
60
40
20
0
(b)
Events / 0.05 GeV/c^2
1
1.2
1.4
1.6
1.8
$M_{K^+K^-}$ (GeV/c^2)
6578A4

Fig. 4

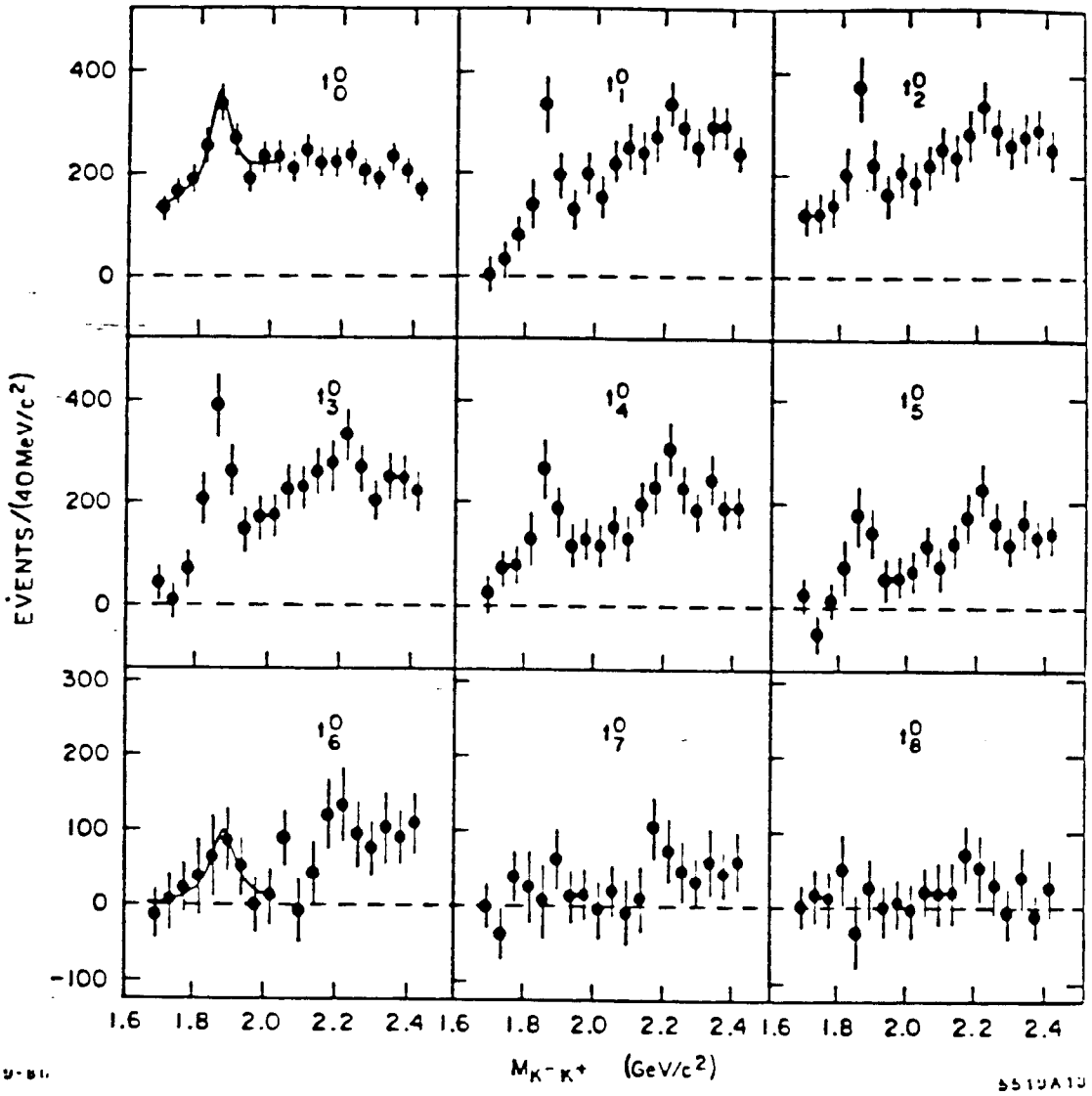
1^0_0
1^0_1
1^0_2
1^0_3
1^0_4
1^0_5
1^0_6
1^0_7
1^0_8
EVENTS/(40MeV/c²)
$M_{K^-K^+}$ (GeV/c²)
1.6
1.8
2.0
2.2
2.4

Fig. 5

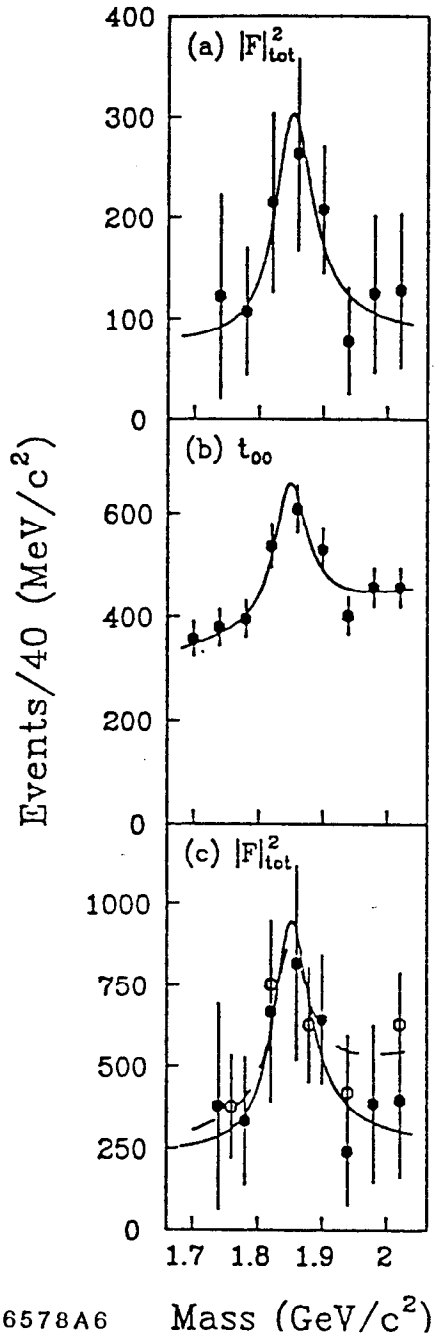

Fig. 6

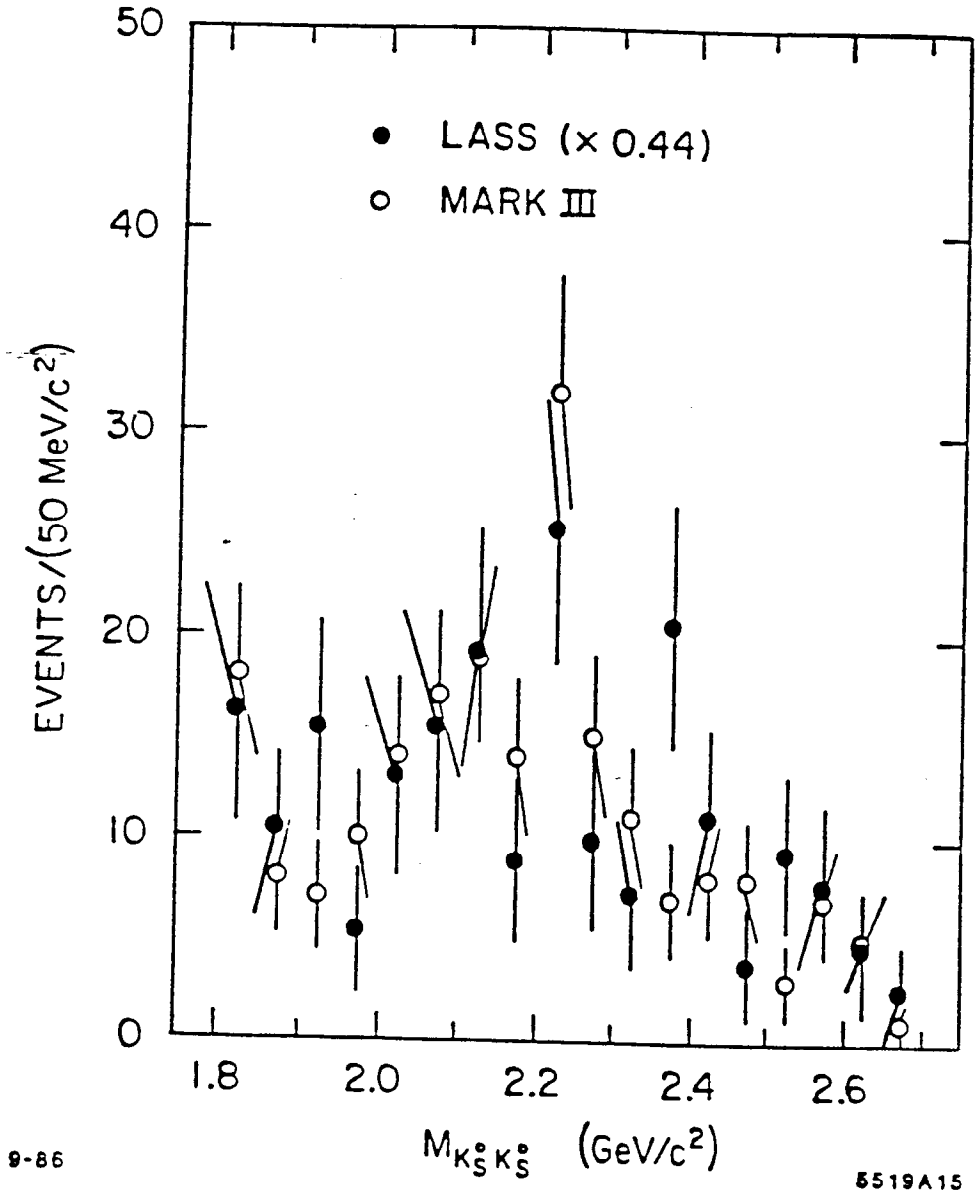

Fig. 7

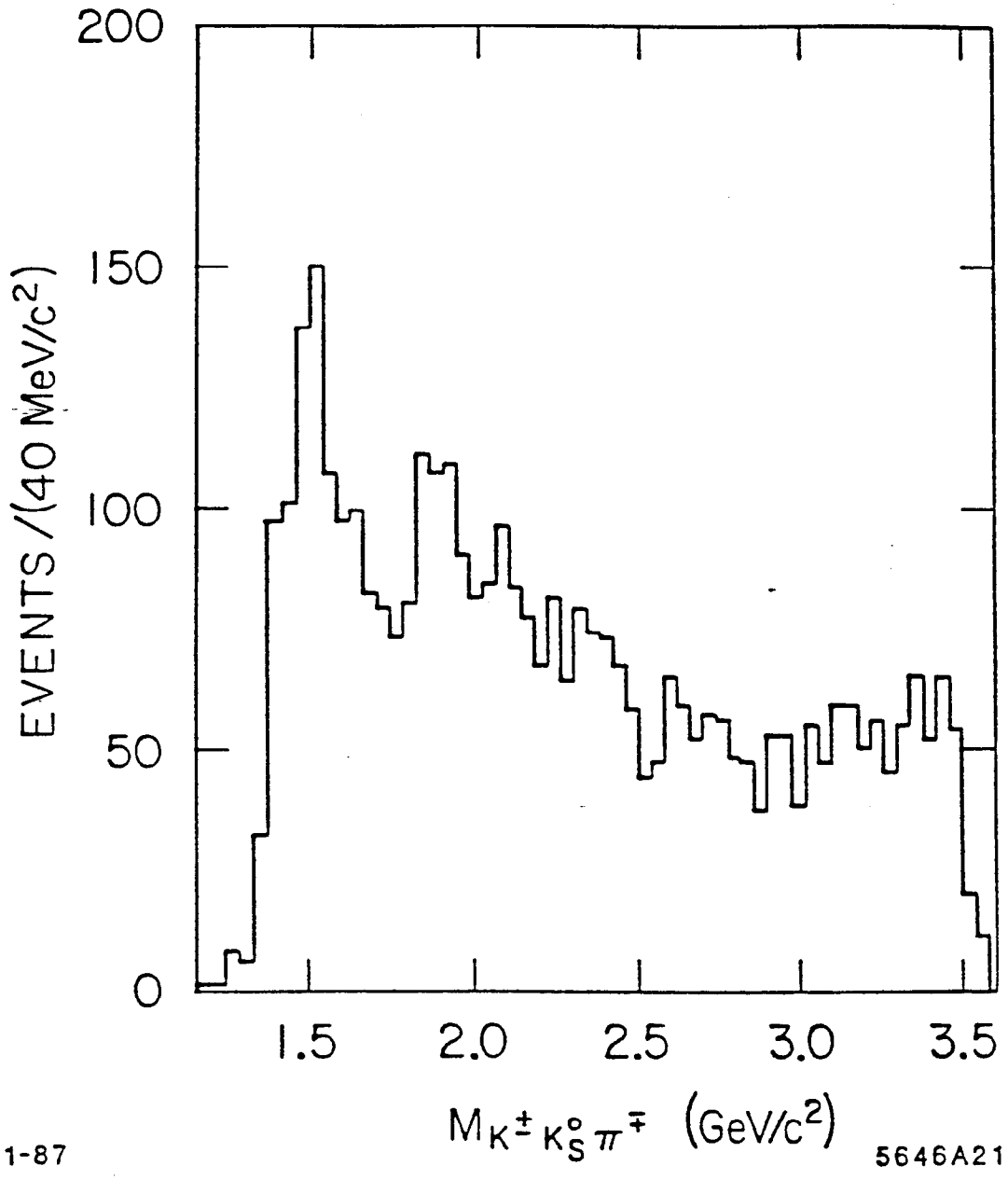
200
150
100
50
0
EVENTS /(40 MeV/c²)
1.5
2.0
2.5
3.0
3.5
$M_{K^\pm K^0_S \pi^\mp}$ (GeV/c²)
1-87
5646A21

Fig. 8

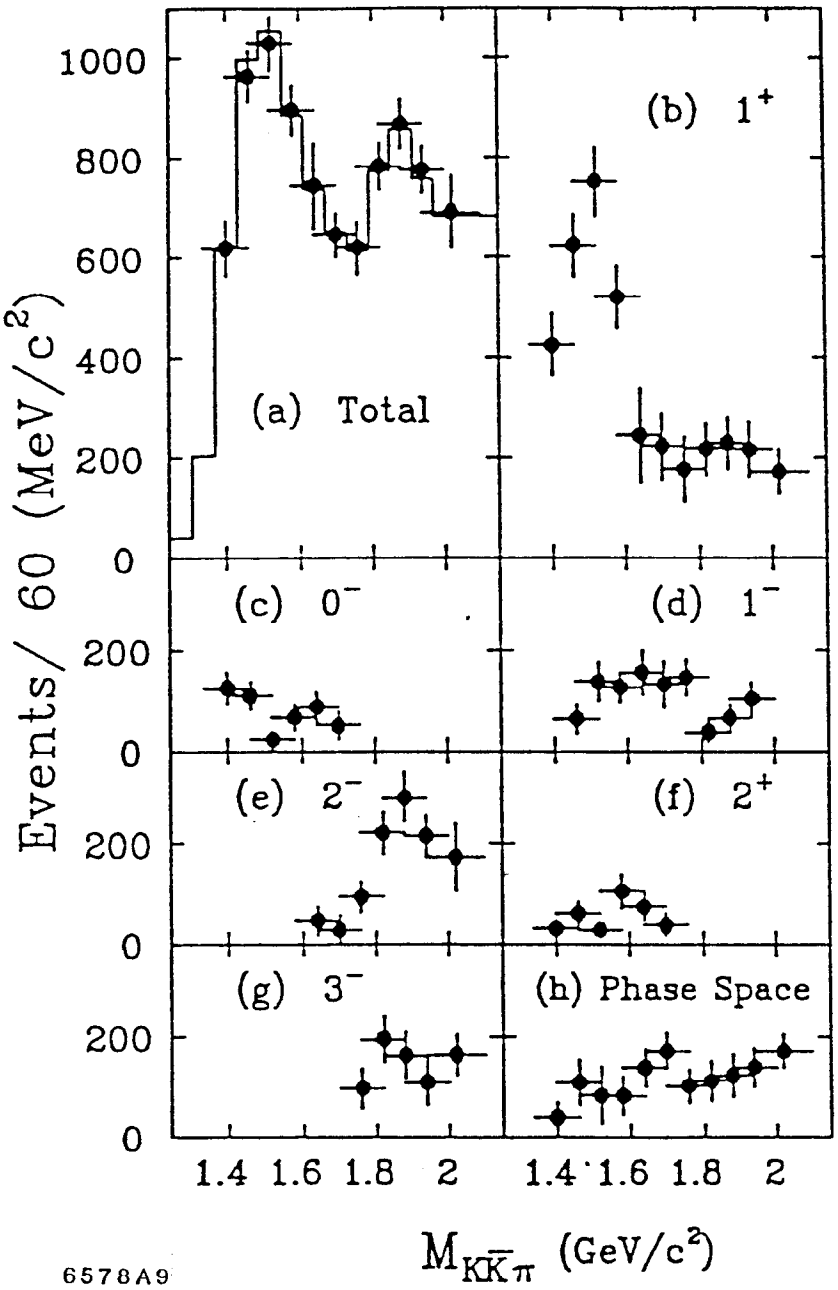
(a) Total
(b) 1+
(c) 0−
(d) 1−
(e) 2−
(f) 2+
(g) 3−
(h) Phase Space
Events/ 60 (MeV/c²)
M_KK̄π (GeV/c²)
6578A9

Fig. 9

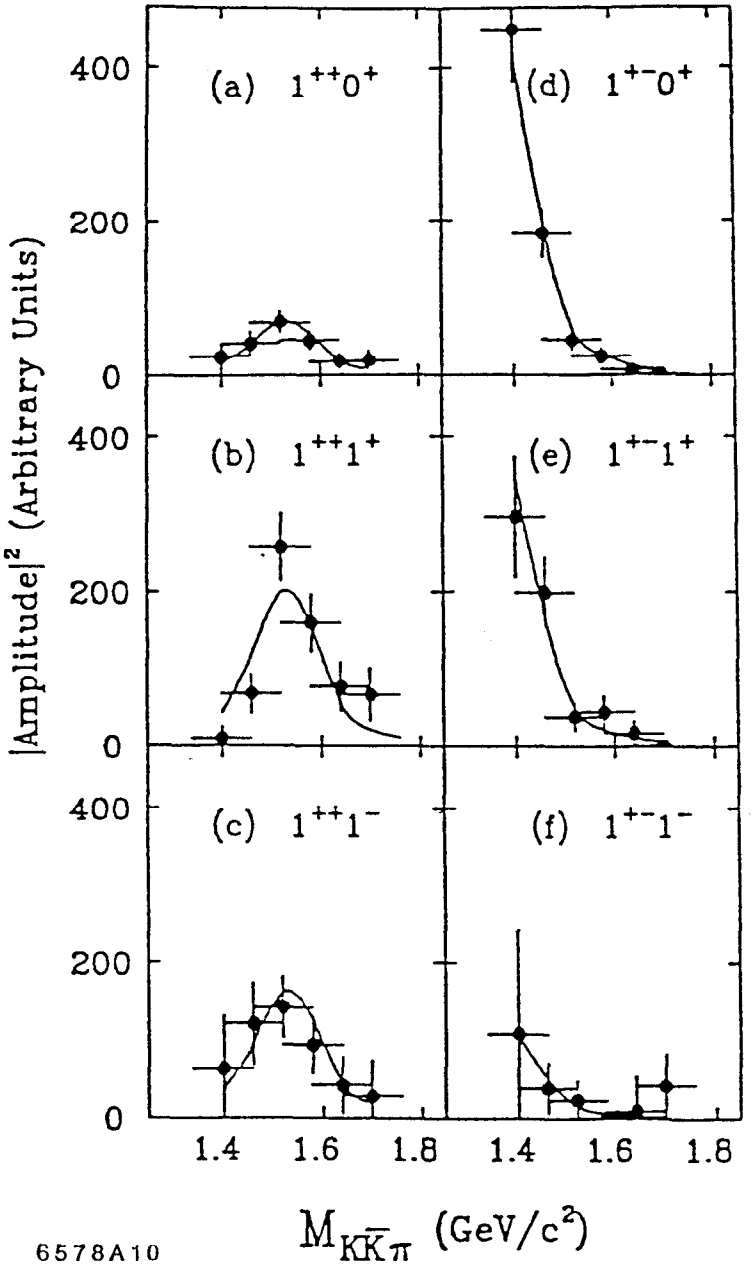
(a) $1^{++}0^+$
(d) $1^{+-}0^+$
(b) $1^{++}1^+$
(e) $1^{+-}1^+$
(c) $1^{++}1^-$
(f) $1^{+-}1^-$
400
200
0
1.4
1.6
1.8
$|\text{Amplitude}|^2$ (Arbitrary Units)
$M_{K\bar{K}\pi}$ (GeV/c^2)
6578A10

Fig. 10